Computational Materials Science 89 (2014) 52–56

Contents lists available at ScienceDirect

Computational Materials Science

journal homepage: www.elsevier.com/locate/commatsci

Thermoelectric properties of Li_2PbGeS_4 polar chalcopyrites single crystals as photovoltaic candidate

Wilayat Khan [a,*], A.H. Reshak [a,b]

[a] New Technologies-Research Center, University of West Bohemia, Univerzitni 8, 306 14 Pilsen, Czech Republic
[b] Center of Excellence Geopolymer and Green Technology, School of Material Engineering, University Malaysia Perlis, 01007 Kangar, Perlis, Malaysia

ARTICLE INFO

Article history:
Received 6 October 2013
Received in revised form 12 March 2014
Accepted 16 March 2014

Keywords:
Seebeck co-efficient
Thermal conductivity
Electrical conductivity
Power factor

ABSTRACT

A theoretical calculation of thermoelectric properties of polar chalcopyrites Li_2PbGeS_4 single crystals is performed in this work. The electronic transport properties are studied using the full-potential linearized augmented plane wave technique (FP-LAPW) and the semi-classical Boltzmann theory under the constant relaxation time for charge carriers and with the deformation potential approximation. The Seebeck co-efficient, electrical conductivity, thermal conductivity and power factor as a function of chemical potential as well as carrier concentration with different temperature is studied. The calculated power factor value shows that Li_2PbGeS_4 crystals is good thermoelectric material in comparison with some well-known thermoelectric materials.

1. Introduction

In recent times there has been a renewed interest in rare-earth chalcogenides [1–5]. The special interests to our research group are rare earth chalcophosphates [6]. These materials consist of a relatively small class of compounds which have been prepared and investigated over the last 3 decades [7–19]. The family of $LnPS_4$ mixtures (where Ln; Y, La, Ce, Pr, Nd, Sm, Gd, Tb, Er, Tm, and Yb) [7] are prominent due to their interesting luminescent behaviors. Low-melting alkali metal polychalcogenide fluxes have proven to be fabulous device for finding out new ternary and quaternary chalcogenides [20,21]. In spite of large number of new compounds discovered with this procedure, synthetic surveys have so far approximately neglected the use of the lighter alkali metals. In general, it is more difficult to get compounds compose of Li and Na because as the size of the alkali metal decreases, the basicity of the flux declines along with the possibilities that the alkali metal will be incorporated in the last product [20]. The Li–S bonds become more covalent and the nucleophilicity of the inoperable S atoms of the S_x^{2-} chains is reduced. In various cases, the Li ion does not get stoichiometrically incorporated into the product, making these fluxes apt for getting alkali metal-free phases. For example, in the Li–Eu–Se system, only $EuSe_2$ could be obtained [22]. However, in several other situations, lithium poly-chalcogenide fluxes useful in incorporating Li^+, yielding new lithium-containing phases such as LiAuS [23,24], Li_3AuS_2 [24], Li_4GeS_4 [25], $Li_{0.5}Pb_{1.75}GeS_4$ [26], and $LiEuPSe_4$ [27]. The new compounds Li_2PbGeS_4 and Li_2EuGeS_4 show another examples in which Li incorporation is successful. They crystallize in the tetragonal non centro-symmetric space assembly I-42 m and possess chalcopyrite-like structure. The literature showed some other mixtures, namely, KAg_2SbS_4 [28] KAg_2AsS_4 [29], $(NH_4)Ag_2–AsS_4$ [30], Ag_2BaGeS_4 [31], Li_2CaGeO_4 and Li_2CaSiO_4 [32]. In the past decade, the ternary chalcopyrite 136_4 [33] semiconductors have arrived into distinction because of their potential for nonlinear optics [34] and photovoltaic applications [35].

Here, in the present work we report thermoelectric properties of Li_2PbGeS_4 using BoltzTraP package [38] incorporated in the full-potential linearized augmented plane wave (FP-LAPW) within generalized gradient approximation (GGA) by Perdew, Burke and Ernzerhof (PBE). Using the Boltzmann theory, we have investigated Seebeck co-efficient, electrical conductivity, thermal conductivity and power factor versus chemical potential as well as carrier concentration at different temperature (300–750 K).

The rest of the paper are organized in three parts: (1) in this part of the paper, we discuss briefly the computational methodology, (2) the second part contain result and their corresponding discussions and finally, the last part (3) in which we summarized briefly the entire discussions.

2. Computational method

The calculations were performed using the all-electron-full-potential linearized augmented plane wave (FP-LAPW) method based on density functional theory (DFT). We have used the program

* Corresponding author. Tel.: +420 775 526 684.
E-mail address: walayat76@gmail.com (W. Khan).

http://dx.doi.org/10.1016/j.commatsci.2014.03.028
0927-0256/

package WIEN2K code [36], the relativistic effects are taken into account within the scalar-relativistic approximation. Exchange and correlation potential are described by the generalized gradient approximation (GGA-PBE) of Perdew–Burke–Ernzerhof [37]. We used $R_{MT}K_{MAX} = 7$ to control the size of basis set for the wave functions. The muffin-tin radii R_{MT} are selected to be 2.0 a.u for Li, Pb, Ge and S atoms, respectively. We have used the semi classical theory of the BoltzTraP package [38] and random phase approximation, in order to obtain the thermoelectric properties of Li_2PbGeS_4 compound. We calculated the transport properties like Seebeck co-efficient, electrical conductivity, thermal conductivity and power factor verses the chemical potential and carrier concentration with different temperature.

3. Result and discussion

3.1. Thermoelectric properties

The transport properties of Li_2PbGeS_4 based on the calculated electronic structure are obtained using Boltzmann theory, with the rigid band approximation (RBA) [39,38] to calculate electronic transport properties. This approximation is used broadly for theoretical calculation of thermoelectric materials, when the doping level is not to high [38–41]. The thermoelectric power $S^2\sigma/\tau$, electrical conductivity σ/τ and thermal conductivity κ/τ are calculated under constant relaxation time. The materials which have greater value of Seebeck co-efficient S, high electrical conductivity σ exhibit low thermal conductivity κ, which is expressed as; $\kappa = \kappa_{el} + \kappa_l$, where κ_{el} represents the electronic thermal conductivity and κ_l represents the lattice thermal conductivity, respectively. Generally, the Wiendemann–Franz law connected the electrical conductivity σ and electronic part of thermal conductivity κ_{el}, i.e. $L(T) = \kappa/\sigma T$. Our investigated compound Li_2PbGeS_4 has semiconducting nature possess band gap of 2.29 eV, which is very close to the experimental band gap (2.41 eV), and show good result as compared to Kanatzidis et al. [42] work, due to which we can use this compounds for thermoelectric properties.

We should emphasize that the lattice thermal conductivity κ_l, caused by the phonon scattering is not considered in these calculations. In such compounds the increase in the scattering of phonon results a decreases the lattice thermal conductivity κ_l.

To know the thermoelectric properties of Li_2PbGeS_4, we calculated and discussed the electronic transport properties in details. In Fig. 1, we plot the Seebeck co-efficient S, thermal conductivity κ, electrical conductivity σ and power factor $S^2\sigma$ as a function of chemical potential $(\mu - E_f)$, at different values of temperatures, where the curve below 0.0 represents the valence band maximum (VBM) and the curve above represent the conduction band minimum (CBM) along the chemical potential $(\mu - E_f)$ respectively.

Fig. 1a, shows the average value of Seebeck co-efficient (S^{ave}/τ) as a function of chemical potential $(\mu - E_f)$ at different temperatures from 300 K to 750 K. The contribution of charge carrier is determined from the sign of the Seebeck co-efficient (S^{ave}/τ), which dominate the transport of electronic charge carriers in the compounds. Mathematically, the Seebeck co-efficient is determined by using the following equation [38]:

$$S_{ij} = E_i(\nabla_j T)^{-1} = (\sigma_{\alpha i})^{-1} V_{\alpha j} \tag{1}$$

For given temperature gradient (∇T), the Seebeck co-efficient possess greater value, which lead to greater value of efficiency of the material.

Fig. 1a, indicates that at four different temperatures (300–750 K), the S^{ave}/τ exhibits variations with respect to chemical potential and also due to the variations in temperature, there is a shift in the Seebeck co-efficient (S^{ave}/τ) toward the CBM. The calculated Seebeck co-efficient of the investigated semiconducting material Li_2PbGeS_4 depicts greater value at low temperature (300 K), as shown in Fig. 1a, and then tends to decrease with temperature because temperature affect the number of carrier concentration i.e. the number of carrier concentration increases with temperature which result a decrease in the Seebeck co-efficient (S^{ave}/τ). It is clear from Fig. 1a, that both electron doping region as well as hole doping region has the same contribution to Seebeck co-efficient (S^{ave}/τ). We plotted the average value of power factor $((S^2\sigma)^{ave}/\tau)$ versus chemical potential $(\mu - E_f)$ at different temperature ranging from 300 to 750 K (Fig. 1b). One can see from Fig. 1b, that there are two prominent peaks around the Fermi level, which presents higher value of thermoelectric performance of Li_2PbGeS_4 compound, with suitable amount of doping [43]. The power factor $((S^2\sigma)^{ave}/\tau)$ at higher temperature (750 K) presents greater values, result from the greater value of carrier concentration, as depicted in Fig. 1b. It is obvious from Fig. 1b, that $(S^2\sigma)^{ave}/\tau$ has bigger value in the electrons doping region as compared to the holes doping region. In the electron doping region, the $(S^2\sigma)^{ave}/\tau$ reaches to its maximum value at 1.7 eV, at temperature 750 K. The same behavior of the $(S^2\sigma)^{ave}/\tau$ is also observed for temperature 300 K, 450 K and 600 K as shown in Fig. 1b. The major peaks of $(S^2\sigma)^{ave}/\tau$ is due to the increase in temperature alone the entire energy region and the peaks around the Fermi energy level move away from the Fermi energy level. Fig. 1b, clarify that n-type doped region is more suitable than p-type doped region in Li_2PbGeS_4.

Fig. 1(c and d), shows the average values of electrical conductivity (σ^{ave}/τ) and the electronic thermal conductivity (κ^{ave}/τ) over relaxation time versus chemical potential $(\mu - E_f)$ for different temperatures. The electrical conductivity (σ^{ave}/τ) depicts two main peaks away from the Fermi level for each value of temperatures ranging from 300 to 750 K, which presents maximum values i.e. $16.5 \times 10^{19}\ (\Omega\ \mathrm{ms})^{-1}$ and $26.5 \times 10^{19}\ (\Omega\ \mathrm{ms})^{-1}$ at low temperature (300 K) situated at −0.133 eV and 0.262 eV. Due to the increase in temperature, the electrical conductivity depicts the decrease in the values. Fig. 1c, depicts that in the conduction band, the value of conductivity along c-axis (principal axis) is larger than the a/b-axes above the conduction band minimum. The electrical conductivity shows weak anisotropy but in thermal conductivity a considerable anisotropy for all mention temperatures has been observed (Fig. 1(c and d). On the other hand, κ^{ave}/τ increases due to the increase in temperature in the given range of chemical potential is clearly shown in Fig. 1d. It is obvious from Fig. 1d, that κ^{ave}/τ is greater for both n-type and p-type doped region of Li_2PbGeS_4 at temperature 750 K as compared to the remaining three values of temperatures.

Here in this work, we also calculated and discussed the electronic transport properties of Li_2PbGeS_4 compound, i.e. Seebeck co-efficient S, the electrical conductivity σ, the electronic thermal conductivity κ_{el} and power factor $S^2\sigma$ as a function of the carrier concentration (cm^{-3}) at four different values of temperatures i.e. 300 K, 450 K, 600 K and 750 K, respectively, as displayed in Fig. 2. Both Fermi–Dirac distribution (FD) and density of state (DOS) are used to find the charge carrier concentration (cm^{-3}).

The hole and electron carrier concentration is given by the following equations:

$$N_p = 2\int_{VB} g(\varepsilon)[1 - f_0(T,\varepsilon,\mu)]\,d\varepsilon \tag{2}$$

$$N_n = 2\int_{CB} g(\varepsilon) f_0(T,\varepsilon,\mu)\,d\varepsilon \tag{3}$$

Fig. 2a, shows the total charge carriers concentration, which is equal to the electrons and holes carriers concentration difference. The net carrier concentration is divided into electrons (n-type doped) and holes (p-type doped). There is small anisotropy in

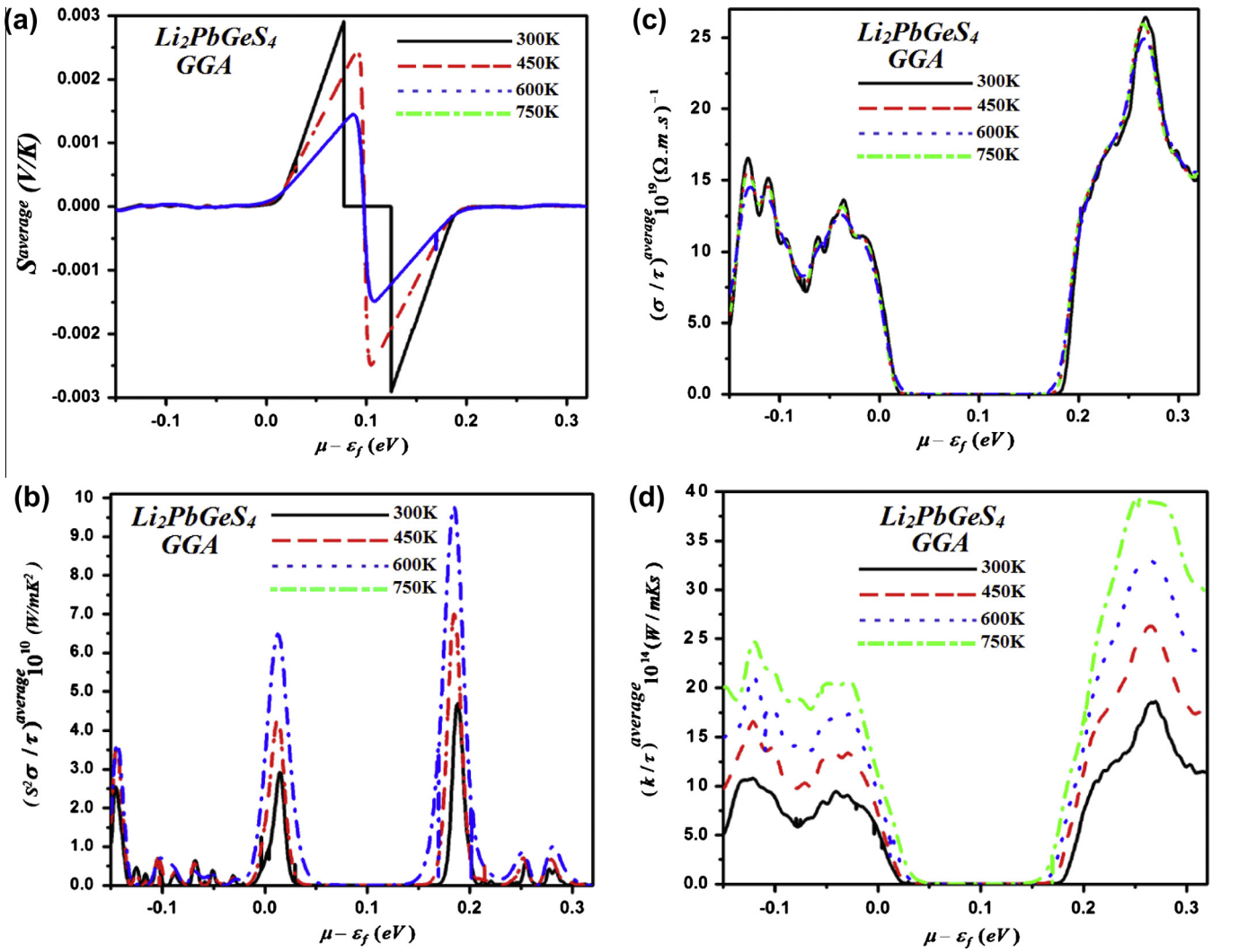

Fig. 1. Calculated transport coefficients of Li_2PbGeS_4 as a function of chemical potential at four different temperatures: Seebeck co-efficient, power factor, electrical conductivity, thermal conductivity.

the electrical conductivity (σ^{ave}/τ) of the Li_2PbGeS_4 compound. The electrical conductivity (σ^{ave}/τ) over relaxation time versus carrier concentration reports linear slope with temperature, resulting from the mobility of charge carriers. From Fig. 2a, it is clear that the mobility of electrons is greater than the mobility of holes with the reason that σ/τ is greater in that region (electrons-doped), which indicate that the investigated compound Li_2PbGeS_4 is *n*-type semiconductor. Once can examine from Fig. 2a, that the transport of electrons is very easy than holes (acoustic phonons scattered holes strongly than electrons), because the valence band is relatively flat and the conduction band is dispersive. It is also clear from Fig. 2a, that the conduction band of Li_2PbGeS_4 is narrower than the valence band. The value of the electrical conductivity σ^{ave}/τ decreases with the increase in temperature (T).

The average value of electronic thermal conductivity (κ^{ave}/τ) over relaxation time is plotted as a function of charge carrier concentration (Fig. 2b), which shows the same behavior as that of electrical conductivity. Thermal conductivity (κ^{ave}/τ) also depends robustly on temperature, as shown in Fig. 2b, which is increases with the increase in temperature and indicates its maximum value at higher temperature (750 K). Thermal conductivity (κ^{ave}/τ) show considerable anisotropy in both regions i.e. in electrons and holes mobility curve. The anharmonicity in lattice vibration result lattice thermal conductivity κ_l, which is characterized by the classical force fields. For such kind of chalcogenides, principal role begin to play electron–phonon anharmonic interactions [44]. The influence of an electron–phonon subsystem on specific heat and two-photon absorption of the semimagnetic semiconductors $Pb_{1-x}Yb_xX$ (X = S, Se, Te) near the semiconductor-isolator phase transformation are studied [45].

We plotted the Seebeck co-efficient (S^{ave}/τ) versus charge carrier concentration for different temperature ranging from 300 to 750 K, which exhibits linear relationship with temperature, as shown in Fig. 2c. The holes indicate positive value and electrons present the negative value of the Seebeck co-efficient (S^{ave}/τ). At Fermi level, there is isotropy in the Seebeck co-efficient (S^{ave}/τ), but around the Fermi level on both sides, there is considerable anisotropy in the Seebeck co-efficient (S^{ave}/τ) (Fig. 2c). In reality, there is linear decrease in (S^{ave}/τ) with chemical potential and exponential increase in carrier concentration, which is explained by the following mathematical relation:

$$S = \frac{8\pi^2 k_B^2}{3eh^2} m^* T \left(\frac{\pi}{3n}\right)^{2/3} \tag{4}$$

The maximum value of the Seebeck co-efficient of the Li_2PbGeS_4 compound ($\pm 3 \times 10^{-4}$ V/K) for both holes and electrons is reported here at temperature 750 K (Fig. 2c). The holes and electrons in (S^{ave}/τ) give similar magnitude.

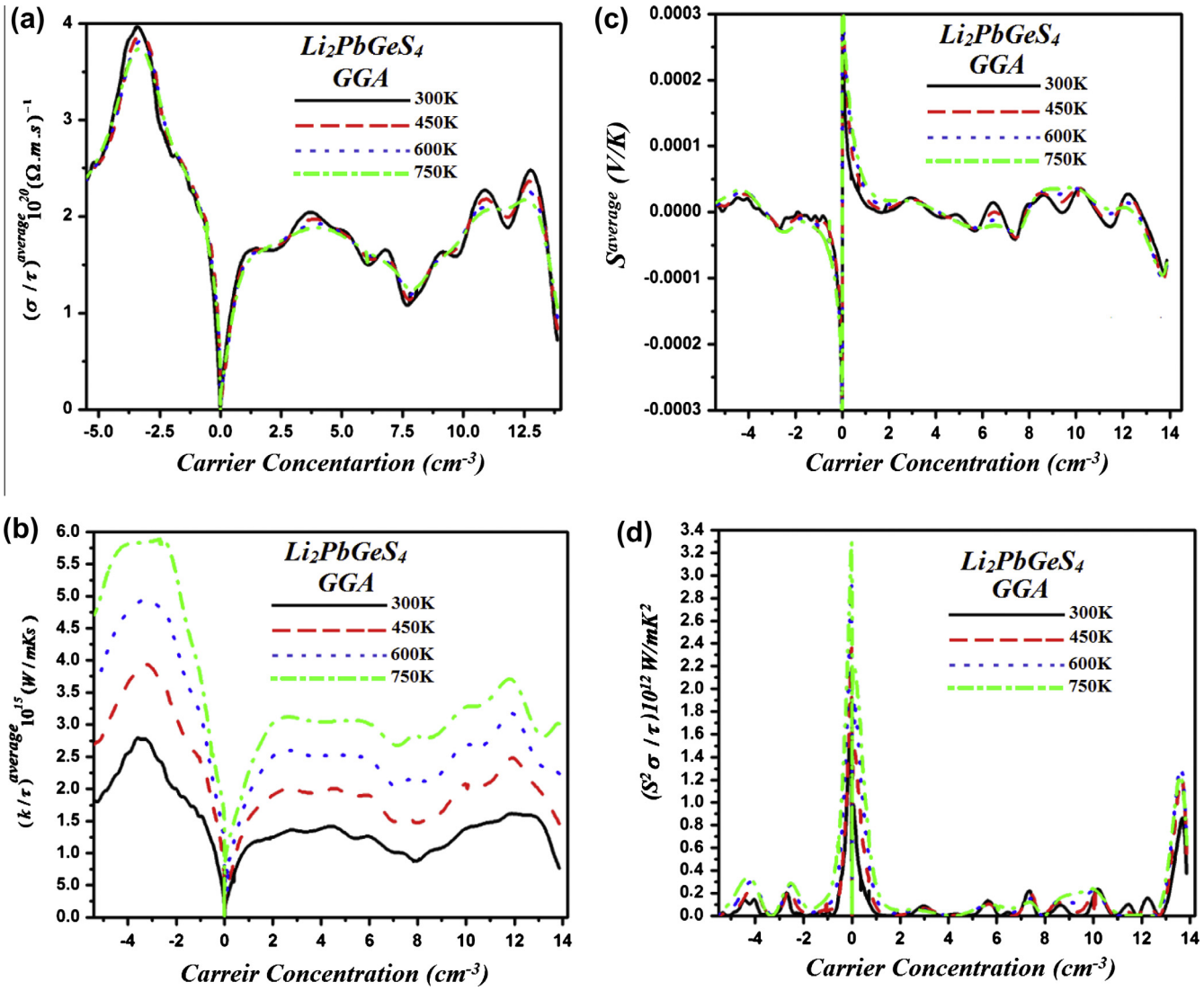

Fig. 2. Calculated transport coefficients of Li_2PbGeS_4 as a function of carrier concentration at four different temperatures: electrical conductivity, thermal conductivity, Seebeck co-efficient and power factor.

Knowing the electrical conductivity and Seebeck co-efficient, then we can find easily the power factor $S^2\sigma/\tau$, which give the exact information about the material efficiency, which is also plotted as function of carrier concentration, as illustrated in Fig. 2d. One can analyze easily from Fig. 2d, that the $(S^2\sigma)^{ave}/\tau$ decreases with the increase in carrier concentration and shows maximum value at certain carrier concentration around Fermi energy level. It should be remembered that the performance of the power factor $S^2\sigma/\tau$ is controlled by doping, which is one of the effective method to control it. Fig. 2d, also predicts that in Li_2PbGeS_4 compound, *n*-type doping is greater than *p*-type doping, proposed that the investigated compound is *n*-type doped thermoelectric material. $(S^2\sigma)^{ave}/\tau$ of Li_2PbGeS_4 has maximum value [46] in the *n*-type doping region (Fig. 2d) than *p*-type doping region. The thermoelectric power factor $S^2\sigma/\tau$ is also strongly depending on temperature, which shows an increase in its value at different ranges of temperature increasing from 300 to 750 K.

4. Conclusions

In conclusion, we investigate the calculated thermoelectric properties of Li_2PbGeS_4 using the full potential linearized augmented plane-wave (PF-LAPW) method and semiclassical Boltzmann theory. The electronic transport properties of this compound, like Seebeck co-efficient, electrical conductivity, thermal conductivity and power factor and their dependence on chemical potential and carrier concentration at different values of temperatures ranging from 300 to 750 K, are studied. Our calculated results depict that electrical conductivity increases due the increase in the number as well as mobility of carrier concentration and decreases with increasing temperature. The calculated thermal conductivity exhibit strong dependence on temperature which increases with temperature and present its maximum value 5.88×10^{15} (W/mK s) at 750 K. The entire calculated results of the Li_2PbGeS_4 show that *n*-type doped region is more suitable for thermoelectric performance than *p*-type doped region. Our calculations also report that the Seebeck co-efficient possess greater value at smaller carrier concentration and vice versa. It should be remember that, we do not consider the charge localization effect or polaron effect in this approach [47]. The results of the power factor also indicate maximum value at certain carrier concentration around Fermi level in the *n*-type doped region, and its magnitude increases with temperature. We calculate maximum power factor and their related doping levels also present that Li_2PbGeS_4 is good thermoelectric materials and exhibit some good thermoelectric performance.

Acknowledgements

This result was developed within the CENTEM project, reg. no. CZ.1.05/2.1.00/03.0088, co-funded by the ERDF as part of the Ministry of Education, Youth and Sports OP RDI program. School of Material Engineering.

References

[1] P.N. Kumta, S.H. Risbud, J. Mater. Sci. 29 (1994) 1135.
[2] I.P. Parkin, J.C. Fitzmaurice, Polyhedron 12 (1993) 1569–1571.
[3] J.H. Chen, P.K. Dorhout, J. Solid State Chem. 117 (1995) 318–322.
[4] L. Iordanidis, M.G. Kanatzidis, Inorg. Chem. 40 (2001) 1878–1887.
[5] F.Q. Huang, J.A. Ibers, J. Solid State Chem. 151 (2000) 317–322.
[6] M.G. Kanatzidis, Curr. Opin. Solid State Mater. Sci. 2 (1997) 139–149.
[7] Z.L. Huang, C. Victoria, M. Pilippe, J. Rare Earth 17 (1999) 6–11.
[8] W. Brockner, R.Z. Becker, Naturforschung 42a (1987) 511–512.
[9] $Eu_2P_2Se_6$ is mentioned briefly as a footnote in Ref. [16b].
[10] W. Carrillo-Cabrera, K. Peters, H.G. von Schnering, Z. Anorg. Allg. Chem. 621 (1995). 557-56.
[11] J.A. Aitken, K. Chondroudis, V.G. Young Jr., Inorg. Chem. 39 (2000) 1525–1533.
[12] K. Chondroudis, T.J. McCarthy, M.G. Kanatzidis, Inorg. Chem. 35 (1996) 840–844.
[13] K. Chondroudis, M.G. Kanatzidis, Inorg. Chem Commun. 1 (2) (1998) 55–57.
[14] K. Chondroudis, M.G. Kanatzidis, Inorg. Chem. 37 (1998) 3792–3797.
[15] P.M.B. Piccoli, K.D. Abney, J.R. Schoonover, P.K. Dorhout, Inorg. Chem. 39 (2000) 2970–2976.
[16] I. Orgzall, B. Lorenz, P.K. Dorhout, P.M. Van Calcar, K. Brister, T. Sander, H.D. Hochheimer, J. Phys. Chem. Solids 61 (2000) 123–134.
[17] C.R. Evenson IV, P.K Dorhout, Inorg. Chem. 40 (2001) 2884–2891.
[18] R.F. Hess, K.D. Abney, J.L. Burris, H.D. Hochheimer, P.K. Dorhout, Inorg. Chem. 40 (2001) 2851–2859.
[19] G. Gautheir, S. Jobic, V. Danaire, R. Brec, M. Evain, Acta Crystallogr. C56 (2000) E117.
[20] M.G. Kanatzidis, Curr. Opin. Solid State Mater. Sci. 2 (2) (1997) 139–149.
[21] M.A. Pell, J.A. Ibers, Chem. Ber. 130 (1997) 1–8.
[22] J.A. Aitken, J.A. Cowen, M.G. Kanatzidis, Chem. Mater. 10 (1998) 3928–3935.
[23] E.A. Axtell, J.H. Liao, M.G. Kanatzidis, Inorg. Chem. 37 (1998) 5583–5587.
[24] F.Q. Huang, Y. Yang, C. Flaschenriem, J.A. Ibers, Inorg. Chem. 40 (2001) 1397–1398.
[25] Y. Matsushita, M.G. Kanatzidis, Z. Naturforsch. 53b (1998) 23–30.
[26] J.A. Aitken, G.A. Marking, M. Evain, L. Iordanidis, M.G. Kanatzidis, J. Solid State Chem. 153 (2000) 158–169.
[27] J.A. Aitken et al., Inorg. Chem. 39 (2000) 1525–1533.
[28] G.L. Schimek, W.T. Pennington, P.T. Wood, J.W. Kolis, J. Solid State Chem. 123 (1996) 277–284.
[29] G.L. Schimek, J.W. Kolis, Acta Crystallogr. C53 (1997) 991–992.
[30] M. Auernhammer, H. Effenberger, E. Irran, F. Pertlik, J. Rosenstingl, J. Solid State Chem. 106 (1993) 421–426.
[31] C.L. Teske, Z. Naturforsch. 34b (1979) 544–547.
[32] J.A. Gard, A.R. West, J. Solid State Chem. 74 (1973) 22–427.
[33] In this notation, the large number represents the number of valence electrons for a particular atom and the subscripted number represents the number of such atoms in the formula.
[34] G.C. Catella, D. Burlage, MRS Bull. 23 (1998) 28–36.
[35] R.W. Birkmire, E. Eser, Annu. Rev. Mater. Sci. 27 (1997) 625–653.
[36] P. Balaha, K. Shewartz, G.K.H. Madsen, D. Kvsnicka, J. Luitz, WIEN2K, an Augmented Plane Wave + Local Orbitals Program for Calculating Crystals Properties, Karlheinz Schewartz, Techn. Universitat, Wien, Austria, 2001, ISBN 3-9501031-1-2.
[37] F. Zerarga et al., Solid State Sci. 13 (2011) 1638.
[38] G.K.H. Madsen, D.J. Singh, Comput. Phys. Commun. 175 (2006) 67.
[39] T.J. Scheidemantel, C. Ambrosch-Draxl, T. Thonhauser, J.V. Badding, J.O. Sofo, Phys. Rev. B 68 (2003) 125210.
[40] L. Chaput, P. Pécheur, J. Tobola, H. Scherrer, Phys. Rev. B 72 (2005) 085126.
[41] X. Gao, K. Uehara, D. Klug, S. Patchkovskii, J. Tse, T. Tritt, Phys. Rev. B 72 (2005) 125202.
[42] M.G. Kanatzidis et al., Chem. Mater. 13 (2001) 4714–4721.
[43] L. Pengfei et al., J. Mater. Sci. 48 (2013) 4999–5004.
[44] K. Nouneh, I.V. Kityk, R. Viennois, S. Benet, K.J. Plucinski, S. Charar, Z. Golacki, S. Paschen, J. Phys. D: Appl. Phys. 38 (2005) 965–973.
[45] K. Nouneh, I.V. Kityk, R. Viennois, S. Benet, S. Charar, S. Paschen, K. Ozga, Phys. Rev. B 73 (2006) 035329.
[46] S. Zhigang, J. Chem. Theory Comput. 8 (2012) 3338–3347.
[47] Y.Y. Wang, J. Zhou, R.G. Yang, J. Phys. Chem. C 115 (2011) 24418–24428.